Med Chem Res
DOI 10.1007/s00044-013-0617-1

MEDICINAL CHEMISTRY RESEARCH

ORIGINAL RESEARCH

DNA-binding and cleavage, cytotoxicity properties of Ru(II) complexes with 2-(4′-chloro-phenyl) imidazo[4,5-*f*][1,10]phenanthroline, ligand and their "light switch" on–off effect

Nazar Mohammed Gabra · Bakheit Mustafa · Yata Praveen Kumar · C. Shobha Devi · M. Shilpa · Kotha Laxma Reddy · S. Satyanarayana

Received: 28 December 2012 / Accepted: 4 May 2013
© Springer Science+Business Media New York 2013

Abstract Three new complexes of the type $[Ru(phen)_2$-PIP-Cl](**1**) $[Ru(bpy)_2PIP-Cl]$(**2**) and $[Ru(dmp)_2PIP-Cl]$ (**3**) (phen = 1,10-phenanthroline; bpy = 2,2′-bipyridine; dmb = 4,4-dimethyl-2,2′-bipyridine), PIP-Cl = 2-(4′-chloro-phenyl) imidazo[4,5-*f*][1,10]phenanthroline) were synthesized and characterized by using UV–VIS, IR and ^{1}H-NMR, ^{13}C-NMR spectral methods. Absorption spectroscopy, emission spectroscopy, viscosity measurements and DNA melting techniques were used to investigate the binding of these Ru(II) complexes with calf thymus DNA, and photocleavage studies were used to investigate the binding of these complexes with plasmid DNA. The spectroscopic studies together with viscosity measurements and DNA melting studies supported fact that Ru(II) complexes bind to CT-DNA(calf thymus DNA) by an intercalation mode via PIP-Cl into the base pairs of DNA. Upon irradiation, these novel Ru(II) complexes cleave the plasmid pBR 322 DNA from the supercoiled form I to the open circular form II.

Keywords Polypyridyl complex · Photocleavage · In vitro cytotoxicity · Docking

N. M. Gabra · B. Mustafa · Y. P. Kumar · C. Shobha Devi · M. Shilpa · K. L. Reddy · S. Satyanarayana (✉)
Department of Chemistry, Osmania University, Hyderabad 500007, Andhra Pradesh, India
e-mail: ssnsirasani@gmail.com

N. M. Gabra
Department of Chemistry, Red Sea University, P.O. Box 24, Port Sudan, Sudan
e-mail: nazargabra@yahoo.com

Introduction

Considerable attention has been given to the design of small molecules that bind to DNA with site selectivity so as to develop new therapeutics and chemical probes for nucleic acid sites and structure, as well as novel diagnostic agents targeted to the double helical DNA (Jenkins *et al*., 1992; He *et al*., 1998). Small molecule serves as analogs in studies of protein-nucleic acid recognition, provides site-specific reagents for molecular biology and yields rationales for new drug design. The effect of size, shape, hydrophobicity and charge on the binding of the complex to DNA has been analyzed by changing the type of heteroaromatic ligand or metal center. In particular, ruthenium (II) complexes with polypyridine ligands, due to a combination of easily constructed rigid chiral structures spanning all three spatial dimensions and a rich photophysical repertoire, have attracted considerable attention. Three types of binding modes, that is, intercalation mode, groove-binding mode and electrostatic-binding mode, have been proposed and further developed to explain the interaction mechanism between the complexes and DNA (Lincoln and Norde'n, 1998; Choi *et al*., 1997; Xiong and Ji, 1999). Although a considerable number of complexes have been reported (Hiort *et al*., 1993; Dupureur and Barton, 1997; Lincoln *et al*., 1996), it is notable that most of them are focused on the prototypes $[Ru(bpy)_2L]^{2+}$ or $[Ru(phen)_2L]^{2+}$ with symmetric intercalative aromatic ligand (L), such as dpq, dppz, pip and their substitution derivates. Recently, some studies on Ru(II) polypyridyl-type complexes with asymmetric aromatic ligand including similar complexes with two Ru(II) atoms have been reported (Zou *et al*., 1999; Deng *et al*., 2003; Jiang, 2004; Jiang *et al*., 2003). However, most of these complexes contain only planar aromatic ligands and investigation of such complexes with ligands containing substituents as DNA-binding reagent is relatively few. In fact, most of

Published online: 26 May 2013

these complexes exhibit interesting properties upon binding to DNA (Barton and Raphael, 1984; Pyle *et al*., 1989; Morgan *et al*., 1991; Xiong *et al*., 1999).

In this paper, we report the synthesis of three complexes of Ru(II) containing a ligand with phenolic and chloro substituents at the 2- and 4-position of the phenyl group, and their binding properties with calf thymus DNA using absorption, fluorescence spectroscopy and viscosity measurements. Their photocleavage behavior toward pBR-233 and the mechanism for cleavage were also investigated. Molecular modeling was carried out to further explore the binding selectivity of duplex oligonucleotides. The result should be of value in understanding the binding mode of the complex to DNA, as well as laying the foundation for the rational design of a DNA molecular light switch and DNA-cleaving agents (Kratochwil *et al*., 1999).

Experimental

Materials

$RuCl_3$, 1,10-phenanthroline monohydrate and 2,2′-bipyridine were purchased from Merck (India). Calf thymus(CT) DNA, 3,4-diaminobenzophenone, 4-chloro-2-(1*H*-imidazo[4,5-*f*][1,10]phenanthroline-2-yl)phenol and 4,4′-dimethyl-2,2′-bipyridine were obtained from Sigma. The supercoiled pBR-322 DNA (Fermentas Life Science, India) was used as received. All other common chemicals and solvents were procured from locally available sources. All the solvents were purified before use as per standard procedures (Perrin *et al*., 1980). Deionized, double-distilled water was used for preparing various buffers. Solutions of DNA in Tris–HCl buffer (pH = 7.2), 50 mM NaCl gave a ratio of UV absorbance at 260 and 280 nm of 1.8–1.9, indicating that the DNA was sufficiently free of protein (Marmur, 1961). The concentration of CT-DNA was determined spectrophotometrically using the molar absorption coefficient 6,600 M^{-1} cm^{-1} (260 nm) (Rreichmann *et al*., 1954).

Synthesis of 2-(4′-chloro-phenyl) imidazo[4,5-f][1,10]phenanthroline (PIP-Cl)

A solution of 1,10-phenanthroline-5,6-dione (0.53 g, 2.50 mmol), 5-chloro-2-hydroxybenzaldehyde (0.547 g, 3.50 mmol) and ammonium acetate in 10 ml glacial acetic acid were refluxed together for 2 h as per Steck and Day (Tan *et al*., 2005) and then cooled to room temperature and diluted with water 25 cm^3. Dropwise addition of liquor ammonia gave a yellow precipitate which was collected washed with water, purified and dried, yield (72 %),

Analytical data Anal. Calcd $C_{19}H_{11}N_4$ for (%) C: 65.81; H: 3.20; N: 16.16; found C: 65.73; H: 3.12; N: 15.98; LC-MS in DMSO M/Z: 347.5 ^{1}H-NMR (DMSO-d_6, 400 MH_Z δ ppm): 9.10 (d, 2H), 8.80 (d, 2H), 8.25 (d, 2H), 7.70 (m, 2H), 7.53 (d, 2H), 7.25(s, 1H),7.10 (d,2H), 6.90 (s, 1H), 6.65 (d, 2H). ^{13}C-NMR (200 MHz, DMSO-d_6, 298 K, δ ppm): 156.36 (C-k), 154.33 (C-i), 152.99 (C-a), 146.72 (C–c), 132.81 (C-e), 131.25 (C-m), 129.49 (C-o), 128.29 (C-d, C-n), 125.06 (C-g), 122.84 (C-b, C-f), 121.85 (C-j), 118.23 (C-l).

Synthesis of [Ru(phen)$_2$ PIP-Cl](ClO$_4$)$_2$·2H$_2$O

A mixture of *cis*-[Ru(phen)$_2$(Cl)$_2$]·2H_2O (0.10 g, 0.16 mmol) and Cl-PIP (0.079 g, 0.16 mmol) in ethanol (30 ml) was refluxed under nitrogen for 8 h. After cooling, the clear solution was filtered. The filtrate was treated with a saturated solution of $NaClO_4$, and a red precipitate was obtained. The solid was collected washed with small amounts of water, ethanol and diethyl ether and then dried under vacuum, yield (69 %),

Analytical data for $RuC_{43}H_{27}N_9Cl_3O_{11}$ Calcd. (%) C: 63.83; H: 3.42; N: 13.75. Found: C: 63.90; H: 3.37; N: 13.86. LC-MS in DMSO M/Z: 1071.5. IR: 1484 (C=C), 1627 (C=N), 722 (Ru–N(L)), 627 cm^{-1} (Ru–N(PIP-Cl). ^{1}H-NMR (DMSO-d_6, 400 MH_Z δ ppm): 9.13 (d, 2H), 8.79 (d, 4H), 8.40 (s, 3H), 8.16 (d, 4H), 8.09 (d, 2H), 8.04 (d, 2H),7.70 (t,2H), 7.45 (d, 2H), 7.15 (d, 2H). ^{13}C-NMR (200 MHz, DMSO-d_6, 298 K, δ ppm): 156.51 (C-k), 153.28 (C-i), 151.21 (C-e) 150.86 (C-1, C-a), 147.85 (C-5), 146.17 (C-3,C–c), 137.27 (C-m, C-4), 131.61 (C-o), 131.00 (C-d), 128.35 (C-6, C-n), 127.72 (C-g), 126.65 (C-f), 123.64 (C-2, C-b), 119.58 (C-l, C-j).

Synthesis of [Ru(bpy)$_2$ PIP-Cl](ClO$_4$)$_2$·2H$_2$O

This complex was synthesized using the same procedure described for complex (**1**) yield (58 %).

Analytical data for $RuC_{39}H_{27}N_8Cl_3O_{11}$: Calcd. (%) C: 63.90; H: 3.37; N: 13.86. Found: C: 63.96; H: 3.35; N: 13.90. LCMS in DMSO M/Z: 1023.5. IR: 1466 (C=C), 1603 (C=N), 768 (Ru–N(L)), 627 cm^{-1} (Ru–N(PIP-Cl)). ^{1}H-NMR (DMSO-d_6, 400 MH_Z δ ppm): 9.10 (d, 2H), 8.90 (m, 2H), 8.25 (t, 3H), 8.66 (t, 3H), 8.12 (m, 4H), 8.08 (d, 2H), 7.93 (t,2H), 7.65 (t,2H), 7.42 (m, 2H), 7.13 (d, 1H). ^{13}C-NMR (200 MHz, DMSO-d_6, 298 K): 157.38 (C-5), 157.16 (C-k), 156.44 (C-i), 151.96 (C-a, C-1), 145.81 (C-e), 138.45 (C-3, C–c), 131.75 (C-m), 128.16 (C-n, C-o C-d), 126.53 (C-g,C-4), 124.93 (C-b, C-f), 123.69 (C-2), 119.64 (C-j), 115.61 (C-l).

Synthesis of [Ru(dmb)$_2$ PIP-Cl](ClO$_4$)$_2$·2H$_2$O

This complex was synthesized using the same procedure described for complex (**1**) yield: 60 %.

Analytical data for $RuC_{43}H_{35}N_8Cl_3O_{11}$: Calcd. (%) C: 63.47; H: 3.99; N: 13.30. Found: C: 63.45; H: 4.15; N: 13.25. LCMS in DMSO M/Z: 1083. IR: 1484 (C=C), 1619 (C=N), 737 (Ru–N(L)), 626 cm^{-1} (Ru–N(pip-Cl). ^{1}H-NMR (DMSO-d$_6$, 400 MH$_Z$ δ ppm): 9.12 (d, 2H), 8.93 (m, 4H), 8.83 (s, 1H), 8.13 (d, 1H), 8.07 (s, 1H), 7.87 (d, 2H), 7.67 (d, 2H), 7.32 (d,2H), 6.98 (m,4H), 2.55 (d, 6H), 2.45 (d,6H). ^{13}C-NMR (200 MHz, DMSO-d$_6$, 298 K): 156.91 (C-5), 156.50 (C-k), 154.53 (C-i), 151.13 (C-a, C-1), 149.59 (C-3), 148.63 (C-e), 145.86 (C–c), 131.20 (C-m), 128.82 (C-o), 126.51 (C-n, C-d), 125.65 (C-4), 124.20 (C-2), 123.77 (C-f), 123.53 (C-g), 123.43 (C-b), 119.47 (C-l), 114.77 (C-j), 21.05 (C-6).

Physical measurements

Microanalyses (C, H, N) were carried out on a *Perkin-Elmer* 240 elemental analyzer. NMR spectra were recorded on Bruker 400 MHz spectrometer with DMSO-d$_6$ as a solvent at room temperature and tetramethylsilane (TMS) as the internal standard. Mass spectra were recorded with LC-MS 2010 A Shimadzu, Japan. IR spectra were recorded, in KBr phase on *Perkin-Elmer FTIR-1605* spectrophotometer. UV–Visible spectra were recorded on *Elico Bio*-spectrophotometer model *BL198*. Emission spectra were carried out with Elico Bio-spectrofluorimeter mode SL174 luminescence spectrometer at room temperature. Spectroscopic titrations were carried out at room temperature to determine the binding affinity between DNA and the complex. Initially, 3 mL solutions of the blank buffer and the ruthenium complexes sample (20 μM) were placed in the reference and sample cuvette (1 cm path length), respectively, and then first spectrum was recorded in the range of 200–600 nm. During the titration, aliquot (1–1 μL) of buffered DNA solution (concentration of ~5–10 mM in base pairs) was added to each cuvette to eliminate the absorbance of DNA itself, and the solutions were mixed for ~5 min; the absorption spectra were recorded. The titration processes were repeated until there was no change in the spectra for four titrations at least; indicating binding saturation had been achieved. The changes in the metal complex concentration due to dilution at the end of each titration were negligible. The above procedure was repeated minimum of three times (Nagababu *et al*., 2011).

Fluorescence emission titration experiments were performed at a fixed metal complex concentration (10 μM) to which DNA (1–160 μM) was added in a volume of (10–100 μL). Excitation wavelength was kept constant, and emission was recorded. Fluorescence emission enhancement was based on comparison of emission intensity at 561 nm of complexes in the absence and presence of CT-DNA.

Viscosity experiments were carried out using an Ostwald viscometer maintained at a constant temperature 30.0 ± 0.1 °C in a thermostatic water bath. Calf thymus DNA samples, approximately 200 base pairs in average length, were prepared by sonicating in order to minimize complexities arising from DNA flexibility (Satyanarayana *et al*., 1993). Data were presented as $(\eta/\eta_0)^{1/3}$ versus the concentration of Ru(II) complexes, where η is the viscosity of DNA in the presence of complexes and η_0 is the viscosity of DNA alone. Viscosity values were calculated from the observed flow time of DNA-containing solutions ($t > 100$ s) corrected for the flow time of buffer alone (t_0) (Moucheron *et al*., 1997; Ashwini Kumar *et al*., 2010).

The DNA melting experiments were carried out by controlling the temperature of the sample cell with a Shimadzu circulating bath while monitoring the absorbance at 260 nm. For the gel electrophoresis experiments, supercoiled pBR-322 DNA (100 lM) was treated with the Ru(II) complexes in 50 mM Tris–HCl, 18 mM NaCl buffer pH 7.8, and the solutions were then irradiated at room temperature with a UV lamp (365 nm, 10 W). The samples were analyzed by electrophoresis for 1 h at 100 V on a 0.8 % agarose gel in Tris–acetic acid–EDTA buffer, pH 7.2. The gel was stained with 1 μg/mL ethidium bromide and photographed under UV light.

In vitro cytotoxicity assay

Cytotoxicity of complexes 1, 2 and 3 was evaluated by using standard MTT (3-(4,5-dimethylthiazole)-2,5-diphenyltetrazolium bromide) assay (Pyle, 1990). Cells were placed in 96-well microassay culture plates (8×10^3 cells per well) and grown overnight at 37 °C in a 5 % CO_2 incubator. The cytotoxicity was evaluated against a panel of four different human cancer cell lines, namely HeLa (ATCC No. CCL-2) derived from human cervical cancer cells, A549 (ATCC No. CCL-185) derived from human alveolar adenocarcinoma epithelial cells, MDA-MB-231 (ATCC No. HTB-26) and MCF7 (ATCC No. HTB-22) derived from human breast adenocarcinoma cells.

Docking simulations

Molecular docking of synthetic compounds into the three-dimensional X-ray structure of DNA (PDB code: 1Y9H) was carried out using the GOLD (Genetic Optimization for Ligand Docking) software package (version 3.0.1) as implemented through the graphical user interface Silver Descriptor 1.1

The 3D structures of DNA molecules were built and saved in Mol2 format with the aid of the molecular

modeling program Discovery Studio 3.0. These partial charges of Mol2 files were further modified by using the Mercury (version 2.2), so that the charges of the nonpolar hydrogens atoms assigned to the atom to which the hydrogen is attached. The resulting files were saved as pdb files. GOLD DOCK 3.0.1 was employed for all docking calculations. The Silver Descriptor interface program was used to generate the docking input files. Ten runs were generated by using genetic algorithm searches. Automatic settings were used, and the results differing within 1.5 Å in positional root-mean-square deviation (RMSD) were clustered together, and the results of the most favorable free energy of binding were selected as the resultant complex structures.

Results and discussion

Synthesis and characterization

The synthetic routes to the ligand and its Ru(II) complexes 1, 2 and 3 are summarized in Fig. 1. The ligand, PIP-Cl, was prepared by a method similar to that described by Steck and Day [50]. Refluxing of 1,10-phenanthroline-5, 6-dione with the appropriate, mole ratio of 2-(4-chlorophenyl) imidazo[4,5-f][1,10]phenanthroline and ammonium acetate in glacial acetic acid for 2 h produced the desired ligand in high yields. The complexes 1, 2 and 3 were prepared by direct reaction of ligand with appropriate mole ratios of the precursor complexes in ethanol. The desired Ru(II) complexes were isolated as their perchlorates and were purified by column chromatography. Three complexes and ligand PIP-Cl were characterized by ^{1}H, ^{13}C-NMR, IR spectra mass spectroscopy and elemental analysis. In the IR spectrum, two peaks appeared in the region 722 and 627 cm^{-1} which corresponds to M–N stretching of metal ancillary of ligand and metal PIP-Cl ligand.

Absorption spectral studies

The application of electronic absorption spectroscopy in DNA-binding studies is one of the most useful techniques. Complex binding with DNA through intercalation usually

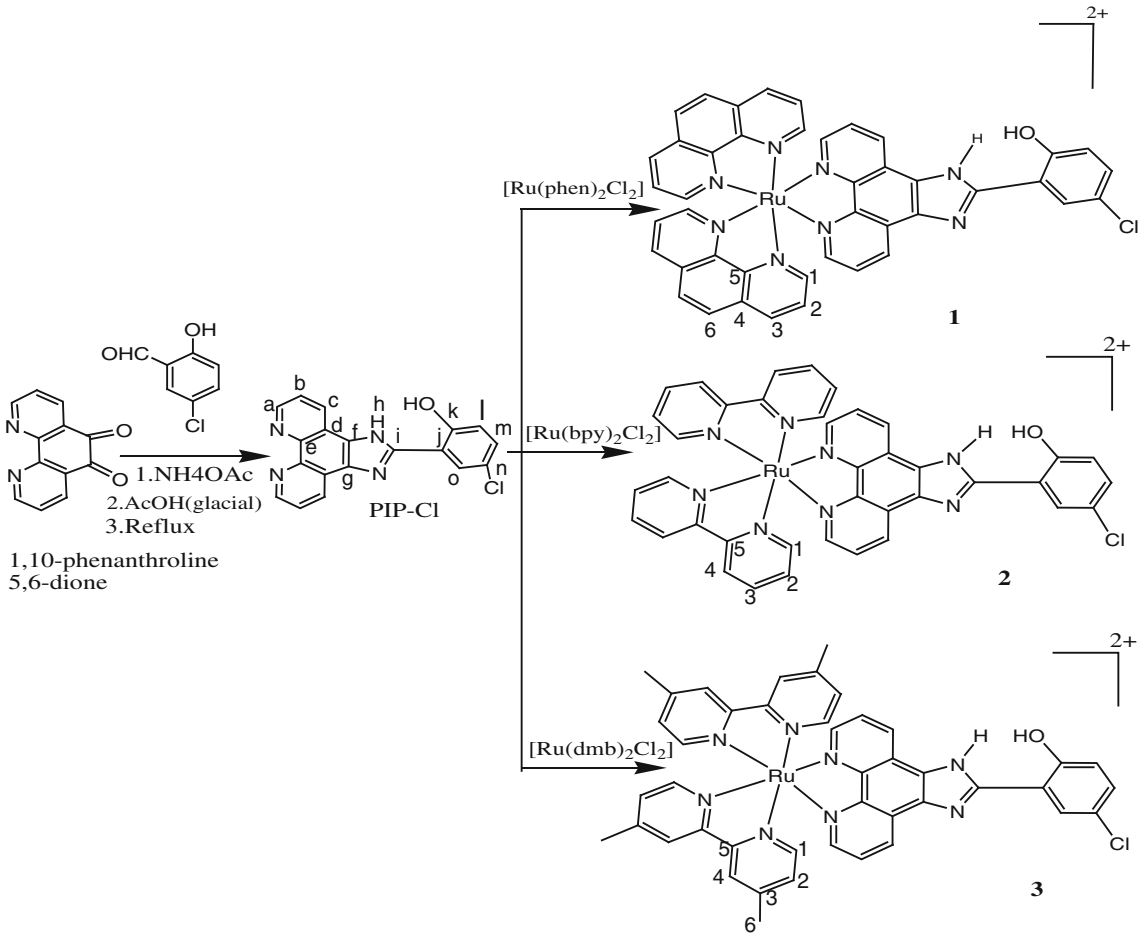

Fig. 1 Synthesis of the complexes $[Ru(phen)_2PIP\text{-}Cl]^{2+}$ (**1**), $[Ru(bpy)_2PIP\text{-}Cl]^{2+}$ (**2**) and $[Ru(dmb)_2PIP\text{-}Cl]^{2+}$ (**3**)

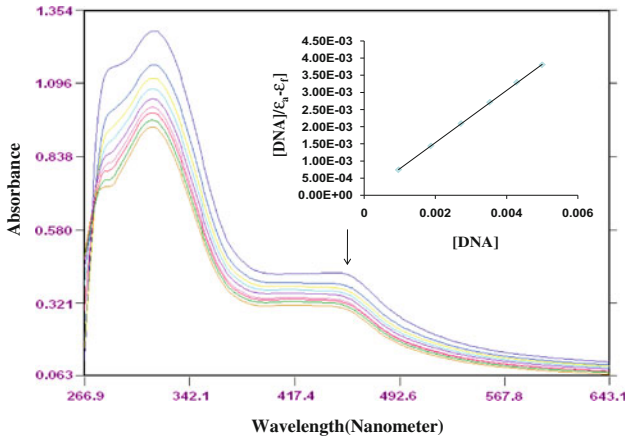

Fig. 2 Absorption spectra of $[Ru(bpy)_2PIP\text{-}Cl]^{2+}$in the absence (*top*) and presence (*lower*) of DNA in Tris–HCl buffer. The absorbance changes upon increasing the CT-DNA concentration (10, 20, 30, 40 μL of DNA addition), [Ru] = 10 μM, [DNA] = 0–126 μM. The *arrow* shows the intensity change upon increasing the DNA concentration. *Inset* plots of $[DNA]/(\sum_a - \sum_f)$ versus [DNA] for the titration of DNA with the Ru(II)

results in hypochromism and bathochromism, because of the intercalative mode involving a stacking interaction between an aromatic chromophore and the base pair of DNA. The extent of the hypochromism commonly parallels the intercalative binding strength. The absorption spectra of complex **2** in the absence and presence of CT-DNA are given in Fig. 2. As increasing the concentration of CT-DNA, the MLCT transition bands of complexes **1, 2** and **3** at 453, 445 and 422 nm exhibit hypochromism of about, 18.5 14.2 and 11.5 % as well as an insignificant bathochromism about 7.2, 6.1 and 5.3 nm, respectively. These results are similar to those reported earlier for various metallointercalators (Pyle, 1990; Wolfe *et al*., 1987). Based on these observations, we presume that there are some interactions between the complexes and the base pairs of DNA. In order to compare quantitatively the binding strength of the three complexes, the intrinsic binding constants K_b of the three complexes with CT-DNA were obtained by monitoring the changes of absorbance in the MLCT band with increasing concentration of DNA using the following equation (Zhen *et al*., 1999) through a plot of $[DNA]/[\varepsilon_a - \varepsilon_f]$ versus [DNA].

$$[DNA]/(\varepsilon_a - \varepsilon_{f)} = [DNA]/(\varepsilon_b - \varepsilon_{f)} + 1/K_b(\varepsilon_b - \varepsilon_f)$$

where [DNA] is the concentration of DNA in base pairs, the apparent absorption coefficients ε_a, ε_f and ε_b correspond to $A_{obsd/[Ru(II)]}$, the extinction coefficients for the free Ru(II) complex, extinction coefficients of complex in the presence of DNA and the extinction coefficients for the Ru(II) complex in the fully bound form, respectively. In plots $[DNA]/(\varepsilon_a - \varepsilon_f)$ versus [DNA], K is given by the ratio of slope to intercept. Intrinsic binding constants K_b of $[Ru(phen)_2PIP\text{-}Cl]^{2+}$(**1**), $[Ru(bpy)\ PIP\text{-}Cl]^{2+}$(**2**) and $[Ru(dmb)_2\ PIP\text{-}Cl]^{2+}$(**3**) were obtained about 6.4×10^5, 4.2×10^5 and 2.1×10^5, respectively (Table 1). The values are comparable with those of some known DNA intercalators, such as $[Ru(phen)_2\ fyip]^{2+}$, $[Ru(bpy)_2\ fyip]^{2+}$ (Shilpa *et al*., 2011;Devi *et al*., 2012;Yata *et al*., 2012). These spectral characteristics of the large hypochromism and clear red shift as well as the large K_b value observed suggest that complexes most likely intercalatively bind to DNA, involving a strong stacking interaction between the aromatic chromophore and the base pairs of DNA. The difference in binding strength of complexes **1** and **2** is probably caused by the different ancillary ligands. The four additional methyl groups in complex **3** relative to complex **2** exert some steric hindrance. Therefore, complex **1** is probably more deeply interacted and more tightly bound to the adjacent DNA base pairs than complex **2**. Similarly, the difference in binding strength of complexes **1** and **3** is due to the difference in the ancillary ligands. On going from phen to dmb, the planarity area and hydrophobicity decrease, leading to a lower binding affinity. The DNA-binding affinities of these complexes follow the order: $[Ru(phen)_2PIP\text{-}Cl]^{2+}$(**1**) > $[Ru(bpy)_2PIP\text{-}Cl]^{2+}$(**2**) > $[Ru(dmb)_2PIP\text{-}Cl]^{2+}$(**3**).

Fluorescence spectroscopic studies

Luminescence spectroscopy is one of the most common and at the same time most sensitive ways to analyze drug–DNA interactions. Support for the above intercalative binding mode also comes from the emission measurement of the complexes. In the absence of DNA, complexes **1, 2** and **3** can emit luminescence in Tris buffer at ambient temperature with maxima at 560 nm. Binding of the three complexes to DNA was found to increase the fluorescence intensity. The results of emission titration for the complex **1** in the absence and presence of CT-DNA are shown in

Table 1 Results of DNA-binding data of Ru(II) complexes

Complex	T_m	Hypochromicity (%)	Absorption λ_{max} (nm) free bound	$\Delta\lambda$ (nm)	K_b
$[Ru(phen)_2PIP\text{-}Cl]^{2+}$ (**1**)	70	14.2	416–422	6	6.4×10^5
$[Ru(bpy)_2PIP\text{-}Cl]^{2+}$ (**2**)	64	18.5	447–453	7	4.2×10^5
$[Ru(dmb)_2PIP\text{-}Cl]^{2+}$ (**3**)	68	11.5	438–445	7	2.1×10^5

CT-DNA T_m = 60 °C

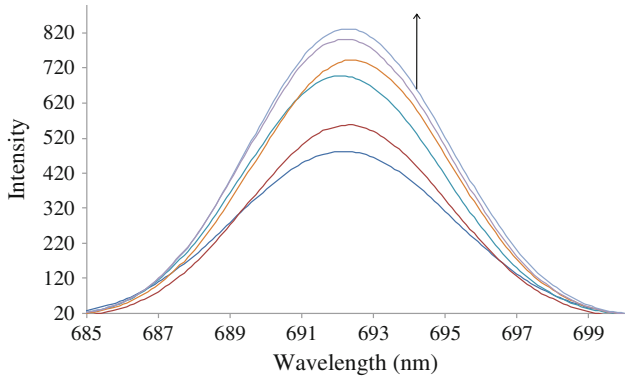

Fig. 3 Emission spectra of complexes of $[Ru(phen)_2PIP\text{-}Cl]^{2+}$ in Tris–HCl buffer at 25 °C upon addition of CT-DNA, [Ru] = 20 μM, [DNA] = 0–120 μM. The *arrow* shows the increase in intensity upon increasing CT-DNA concentrations

Fig. 3. Upon addition of CT-DNA, the emission intensity increases steadily and reaches 1.91 times larger than that in the absence of DNA for complex **1**, 1.30 times larger than that of in the absence of DNA for complex **2** and 1.79 times larger than that of in the absence of DNA for complex **3**, respectively. This implies that these complexes strongly interact with DNA and can be efficiently protected by DNA (Table 2), since the hydrophobic environment inside the DNA helix reduces the accessibility of solvent water. In this way, the mobility of the complexes is restricted at the binding site, leading to a decrease in the vibrational modes of relaxation.

Table 2 Emission data of complexes

Complexes	Ex peak	Em peak	Fluorescence binding constant
$[Ru(phen)_2PIP\text{-}Cl]^{2+}$ (**1**)	468	610	6.9×10^5
$[Ru(bpy)_2PIP\text{-}Cl]^{2+}$ (**2**)	468	691	5.4×10^5
$[Ru(dmb)_2PIP\text{-}Cl]^{2+}$ (**3**)	467	470	1.4×10^5

Differential luminescence quenching was also utilized in monitoring DNA binding. A highly negatively charged

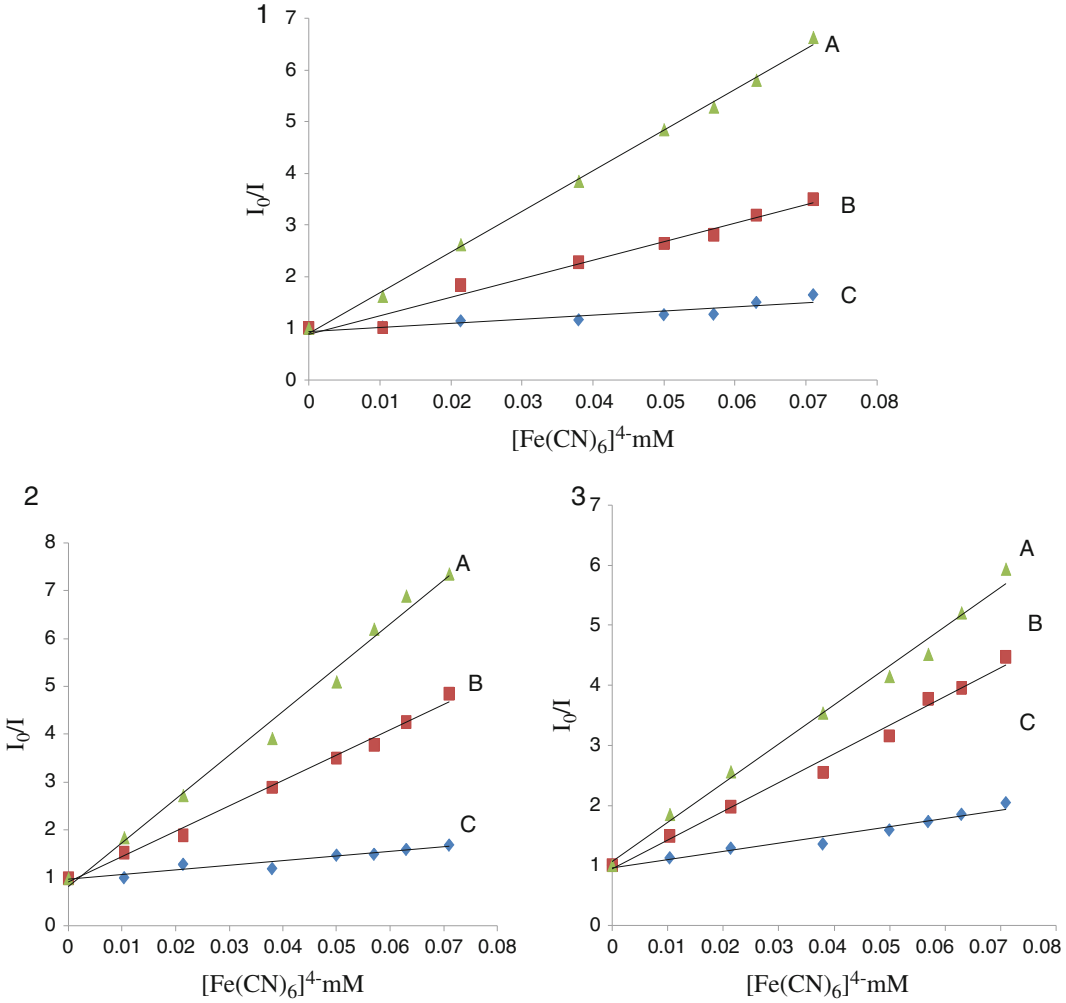

Fig. 4 Emission quenching curves of complexes **1, 2** and **3**. Quenching in the absence of DNA (**a**), quenching in the presence of DNA (**b**) (1:20). Excess of DNA (1:200 μM) (**c**)

quencher is expected to be repelled by the negatively charged phosphate backbone, and therefore, a DNA-bound cationic molecule should be readily quenched (Lakowicz and Webber, 1973). Figure 4 shows the steady-state emission quenching experiments using $[Fe(CN)_6]^{4-}$ as quencher. In the absence of DNA, all three complexes were efficiently quenched by $[Fe(CN)_6]^{4-}$, but when bound to DNA the complexes were protected from the quencher. This may be explained by repulsion between the highly negatively charged $[Fe(CN)_6]^{4-}$ and the DNA polyanion backbone which hinders access of $[Fe(CN)_6]^{4-}$ to the DNA-bound complexes. The quenching studies indicate that the DNA-binding abilities of the complexes follow the order: 1, 3 and 2. Steady-state emission quenching experiments using $[Fe(CN)_6]^{4-}$ as quencher were also used to observe the binding of the complexes with CT-DNA. The Stern–Volmer quenching constant (K_{sv}) can be determined by using Stern–Volmer equation (Satyanarayana *et al.*, 1992).

$$I_0/I = 1 + K_{sv}[Q]$$

where I_0 and I are the intensities of the fluorophore in the absence and presence of quencher, respectively, Q is the concentration of the quencher and K_{sv} is a linear Stern–Volmer quenching constant. In the quenching plot of I_0/I versus $[Q]$, K_{sv} is given by the slope. Figure 4 shows the Stern–Volmer plots for both the free complex in solution and the complex in the presence of increasing amounts of DNA. All the complexes show linear Stern–Volmer plots. The K_{sv} values for the complexes in the absence of DNA were 482, 319 and 272 nm, for complexes (**1**), (**2**) and (**3**), respectively. In the presence of DNA, the Ksv values were 261, 190 and 163 for complexes (**1**), (**2**) and (**3**), respectively. Hence, the K_{sv} values are smaller in the presence of DNA. At high concentration of DNA (1:200; Ru^{2+}: DNA), the plots have essentially zero slope, indicating that the bound species is inaccessible to quencher.

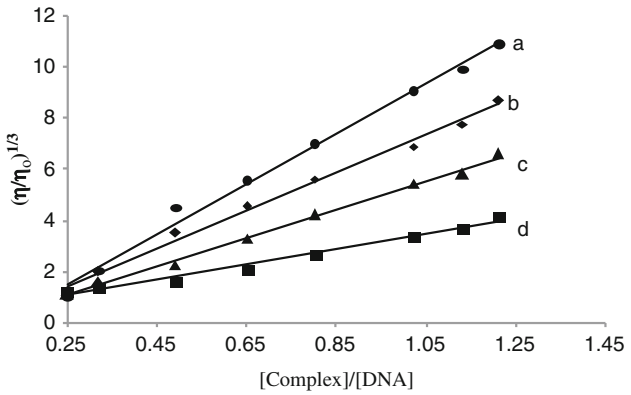

Fig. 5 Effect of increasing amount of complexes on the relative viscosities of CT-DNA at 25 ± 0.1 °C EB (*a*), $[Ru(phen)_2PIP\text{-}Cl]^{2+}$ (*b*), $[Ru(bpy)_2PIP\text{-}Cl]^{2+}$ (*c*) and $[Ru(dmb)_2PIP\text{-}Cl]^{2+}$ (*d*)

Viscosity measurements

Measurement of DNA viscosity is regarded as the least ambiguous and the most essential analysis of the binding mode of DNA in solution, and particularly affords stronger evidence for an intercalative DNA-binding mode. The viscosity changes are the consequence of a change in length of the DNA. A classical intercalator like ethidium bromide reveals a significant increase in the viscosity of the DNA solution, due to an increase in the separation of base pairs at the intercalation sites and hence an enhancement in overall DNA length (Satyanarayana *et al.*, 1993; Lecomte *et al.*, 1992) In contrast, partial or nonintercalation binding modes, such as electrostatic or covalent binding, typically reduce or make no change in the DNA solution viscosity (Arounaguiri and Maiya, 1996). The effects of complexes **1–3** on the viscosity of DNA are shown in Fig. 5. The viscosity of DNA is increased with the increment of each one of complexes **1–3**, and it is similar to the behavior of well-known DNA intercalator ($[Ru(bpy)_2(dppz)]^{2+}$) (Graham *et al.*, 1980), on the other hand, for $[Ru(bpy)_3]^{2+}$, which has also been well known to bind to DNA in an electrostatic mode. There is no effect on the relative viscosity of DNA solution. The increase in viscosity for complexes **1**, **2** and **3** was less compared to the ethidium bromide. The experimental results further support that all the three complexes bind to DNA in an intercalation mode.

Thermal denaturation study

The melting of DNA can be used to distinguish between those molecules which bind via intercalation and those which bind externally. The melting temperature T_m, at which 50 % of the DNA has become single-stranded, can be determined from the thermal denaturation curves of DNA. In the absence of any added complex, the melting transition of CT-DNA was sharp. Intercalation of organic dyes or metallointercalators generally results in a considerable stabilization of the DNA duplex with a corresponding large increase in melting temperature (T_m). In the presence of intercalators, the T_m rises sharply until all the intercalating sites are saturated, after which the stabilization was due to electrostatic binding, and T_m increases less steeply (Haq *et al.*, 1995). Thermal denaturation experiments carried out on CT-DNA in the absence of any added complex revealed that the T_m for the duplex was 60.5 °C under our experimental conditions.

The observed melting temperature in the presence of complexes 1, 2 and 3 was 72.4 ± 0.3, 68.2 ± 0.3, 64.8 ± 0.3, respectively. The experimental results indicate that the complex (**1**) exhibits larger DNA-binding affinity than complex **3**.

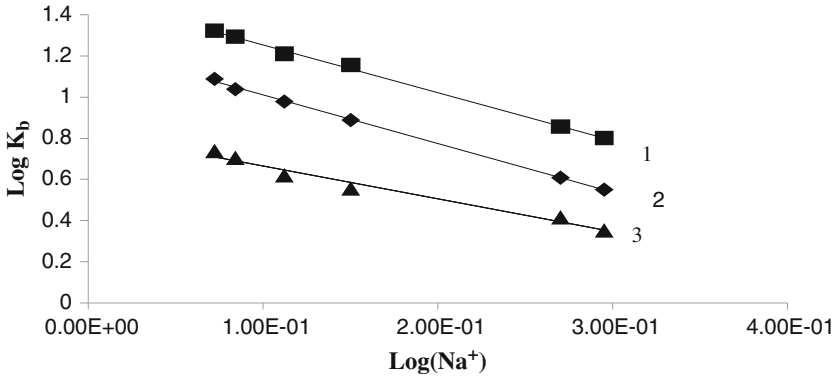

Fig. 6 Salt dependence of the equilibrium binding constants for DNA binding of complexes $[Ru(phen)_2PIP\text{-}Cl]^{2+}$ (**1**), $[Ru(bpy)_2PIP\text{-}Cl]^{2+}$ (**2**) and $[Ru(dmb)_2PIP\text{-}Cl]^{2+}$ (**3**). The lines indicate the slope of the linear square fit to the data as **a** −2.1, **b** −1.86, **c** −1.37

Salt titration

Reverse salt titrations of **1, 2** and **3** bound to DNA were performed, and the results are shown in Fig. 6. The binding constant at each titration point was then calculated, and a plot of log[K_b] versus log[Na^+] was constructed. From polyelectrolyte theory, the slope of this graph provides an estimate of $SK = (\delta \log[K_b]/\delta \log[Na^+]) = Z\psi$, where Z is the charge of the metal complex and ψ is 0.88 for DNA[37,39]. Figure 6 shows the decrease of K_b of **1**, **2 and 3** as the concentration of Na^+ is increased. As expected, the plot becomes nonlinear at ionic strengths greater than 0.1 M (Record *et al*., 1978; Mudasir *et al*., 2006). The slopes of the lines in Fig. 6 are being −2.1, −1.86 and

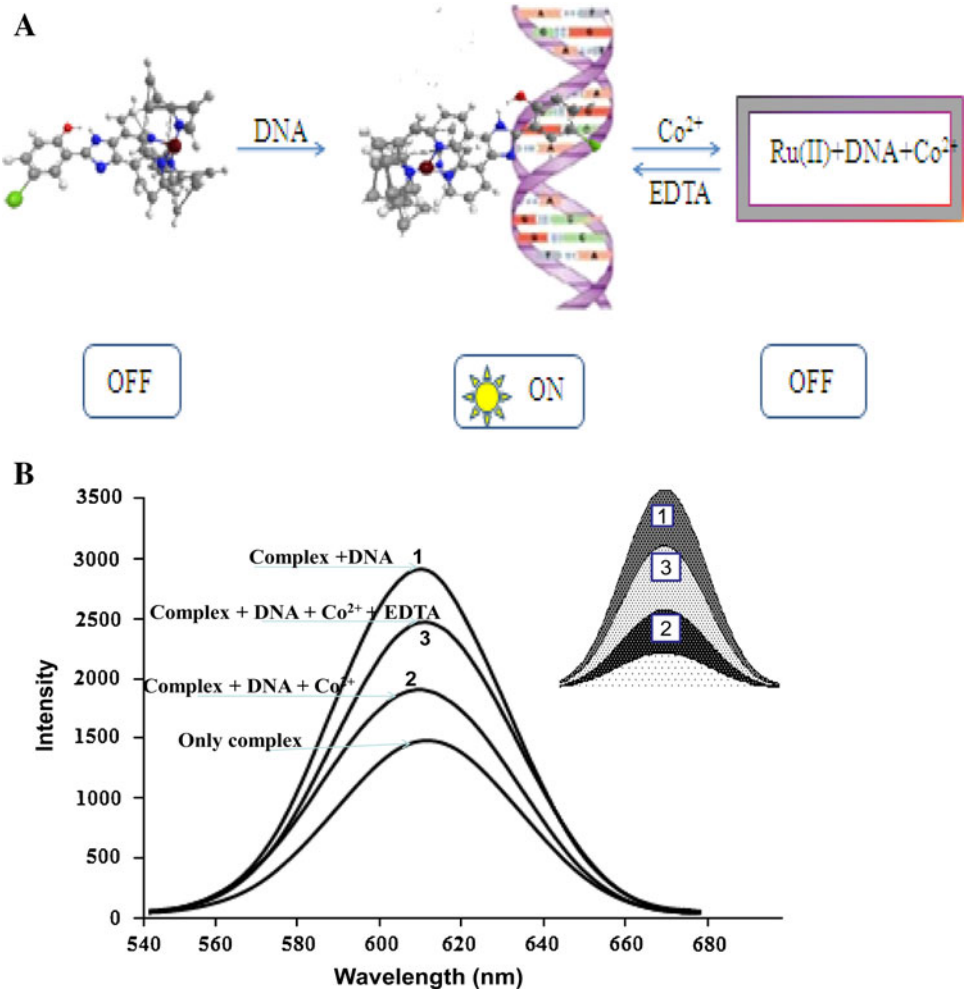

Fig. 7 a, b $[Ru(phen)_2PIP\text{-}Cl]^{2+}$ in Tris buffer (**1**), complex + DNA (**2**), complex + DNA + Co^{2+} (**3**) and complex + DNA + Co^{2+} + EDTA (**4**)

−1.37 for **1**, **2** and **3** complexes, respectively. The values of complexes **1** and **2** are more than the theoretically expected values of $Z\psi$ ($2 \times 0.88 = 1.76$) but complex 3 shows less value. Such lower values could arise from coupled anion release or from change in complex or DNA hydration upon binding (4). The knowledge of $Z\psi$ allows for a quantitative estimation of the nonelectrostatic contribution to the DNA-binding constant for these complexes.

Light switch on–off effect

Ruthenium(II) complexes bind to DNA through the intercalation of the PIP-Cl ligand between the bases of the duplex, resulting in an increase in the luminescence intensity, thus making it a "DNA light switch"(Liu *et al*., 2004). The $[Ru(bpy)_2(Cl\text{-}PIP)]^{2+}$ DNA light switch can be turned off in the presence of Co^{2+}, Ni^{2+} and Zn^{2+}, and the emission can be fully restored by the addition of EDTA. The quenched change in the luminescence intensity of DNA-bound Ru(II) complexes due to the interaction of Co^{2+} with DNA is shown in Fig 7a, b. Cycling of the DNA light switch OFF and ON can be accomplished through the successive introduction of Co^{2+} and EDTA, respectively, to solutions of DNA bound. The luminescence intensities of DNA-bound Ru(II) in the presence of Co^{2+} and EDTA reveal the modulation of Co^{2+} and EDTA to luminescence intensities of DNA-bound Ru(II).

Photoactivated cleavage of pBR 322 DNA

There has been considerable interest in DNA endonucleolytic cleavage reactions that are activated by metal ions (Liu *et al*., 2005; Barton and Raphael, 1984). The delivery of high concentrations of metal ion to the helix, in locally generating oxygen or hydroxide radicals, yields an efficient DNA cleavage reaction. DNA cleavage was monitored by relation of supercoiled circular pBR 322 (Form I) into nicked circular (Form II) and linear (Form III). When circular plasmid DNA was subjected to electrophoresis, relatively fast migration will be observed for the supercoiled form (Form I). If scission occurs on one strand (nicking), the supercoils will relax to generate a slower-moving open circular form (Form II) (Marmur, 1961). If both strands are cleaved, a linear form (Form III) will be generated that migrates between Forms I and II. Figure 8 shows the gel electrophoretic separations of plasmid pBR322 DNA after incubation with Ru(II) complexes and irradiation at 365 nm. Fig. 8 reveals the conversion of varying concentrations of $[Ru(phen)_2PIP\text{-}Cl]^{2+}$, $[Ru(bpy)_2PIP\text{-}Cl]^{2+}$and $[Ru(dmb)_2PIP\text{-}Cl]^{2+}$. It can be seen that with increasing the concentration of $[Ru(phen)_2PIP\text{-}Cl]^{2+}$ and $[Ru(bpy)_2PIP\text{-}Cl]^{2+}$, Form II increases gradually, while Form I diminishes gradually. With increasing irradiation time, Form I of pBR322 DNA diminishes gradually, whereas the amount of Form II increases. This is the result of single-stranded cleavage of pBR 322 DNA. It can also be seen in Fig. 6c that neither irradiation of DNA at

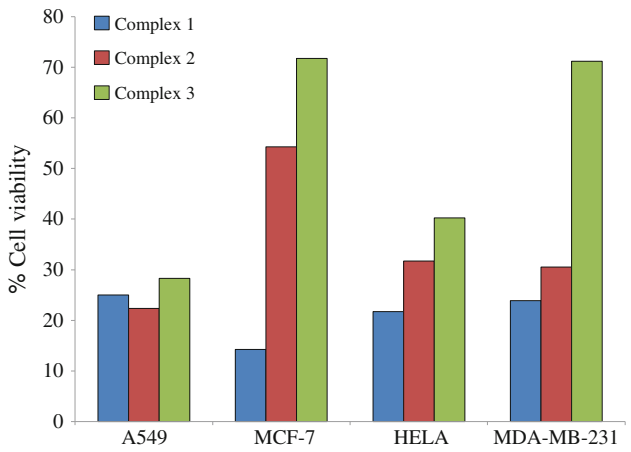

Fig. 9 Percentage cell viability of complexes $[Ru(phen)_2PIP\text{-}Cl]^{2+}$ (**1**), $[Ru(bpy)_2PIP\text{-}Cl]^{2+}$ (**2**) and $[Ru(dmb)_2PIP\text{-}Cl]^{2+}$ (**3**), with different cell lines. Complex concentrations were 25 μM, and cells were incubated for 24 h

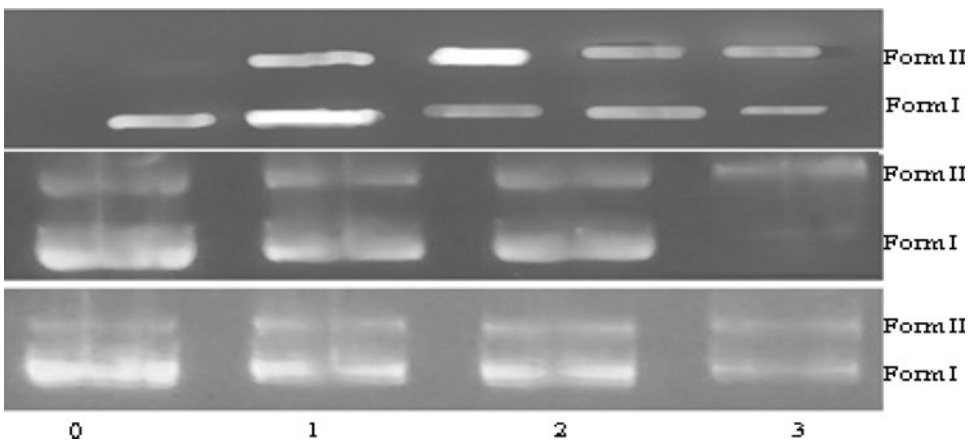

Fig. 8 Photo-activated cleavage of pBR 322 DNA in the presence of $[Ru(phen)_2PIP\text{-}Cl]^{2+}$ (**1**), $[Ru(bpy)_2PIP\text{-}Cl]^{2+}$ (**2**) and $[Ru(dmb)_2PIP\text{-}Cl]^{2+}$ (**3**) complexes, after irradiation at 365 nm. *Lane 0* controls plasmid DNA (untreated pBR 322), *lanes 1–3*, addition of complexes 20, 40 and 60 M^{-1}

Table 3 Percentage cell viability of different cell lines with ruthenium complexes

Complex	A549	MCF-7	HELA	MDA-MB-231
$[Ru(phen)_2PIP\text{-}Cl]^{2+}$ (**1**)	25.03	14.23	21.75	23.88
$[Ru(bpy)_2PIP\text{-}Cl]^{2+}$ (**2**)	22.37	54.3	31.74	30.55
$[Ru(dmb)_2PIP\text{-}Cl]^{2+}$ (**3**)	28.29	71.78	40.21	71.23

365 nm without Ru(II) nor incubation with Ru(II) without light yields significant strand scission. It was likely that the reduction of Ru(II) is the important step leading to DNA cleavage.

In vitro cytotoxic assay

Cytotoxicity was tested for Ru(II) complexes by MTT assay against several selected cell lines depicted in Fig. 9. The following human cancer cell lines were used for the experiment: human cervical cancer (HeLa), human breast adenocarcinoma cell line (MDA-MB-231, MCF-7) and human alveolar adenocarcinoma (A549), and the results were compared to see the differences that might arise from their structural differences. All compounds showed good activity in the **A549** cell line and moderate activity in **MDA-MB-231** cell lines Fig. 9, suggesting the different ancillary ligands have little effect on their activity (Table 3).

A minor difference was also noted for complexes **1** and **2** in HELA cell lines. The complex 3 having dmb ancillary ligand showed very low or no activity at all in the cell lines tested (Table 3), indicating that the methyl group is not important for activity.

From the obtained data, it was clear that the complex **1** was more sensitive against the selected tumor cell lines than complex **2**, but these complexes all exhibited relatively lower in vitro cytotoxicity against the selected cell lines than cisplatin.

Docking studies

For molecular docking of the complex with DNA sequence d(CCATCGCTACC) after satisfactory spectroscopic measurement of DNA-binding study of the complex, molecular docking study was performed to understand the preferred orientation of sterically acceptable complex using Cl-PIP ligand with the DNA sequence. According to this docking experiment, complex reasonably binds with DNA sequence d(CCATCGCTACC). The docking result (Table 4) suggested the best possible conformation of the complexes interaction mainly through phenyl ring inside the DNA major groove. It has been observed that the complex is stabilized by electrostatic hydrogen bonding with DNA bases, particularly involving O atoms on the phosphate of DNA base pairs and N3 of guanine, in addition to van der Waals and stacking bond interactions between electron deficient chloro substituents phenyl ring system and purine–pyrimidine bases coordinated to Ru(II) ion, participates in hydrogen bonding, whereas the side chains attached to Ru(II) complex enabled the molecules to stay in the groove with the help of van der Waals forces. The hydrogen bonding interactions involving the energy-minimized docked poses of d(CCATCGCTACC) with complexes are shown in Table 4. Thus, molecular docking study together with spectroscopic studies indicated that complex 1 interacts with the DNA through both covalent and noncovalent interactions which perhaps owe to its stronger bonding with DNA.

Antimicrobial activity

All the complexes exhibited varying antimicrobial activity toward most of the microbes selected (Table 5) and were found to be dose dependent. Most of the complexes inhibited moderate growth of gram-negative bacteria Escherichia coli (MTCC 443) and gram-positive

Table 4 The H-Bond, van der Waals interaction and scores for binding of Ru(II) and Co(III) complexes to (1y9 h) DNA decamer containing CG bases using docking calculation

Complex	H-bond donor–acceptor	Bond length (Å)	van der Waals interactions (complex DNA)	Bond length (Å)	Docking score
$[Ru(phen)_2PIP\text{-}Cl]$	O54-G13:H21	2.413	H78-DC17:H5	1.852	39.656
	O54-G13:H22	2.658	H66-DG16:H5	1.365	
	H81-DG13:N2	2.555	C35-DC10:OP1	2.456	
	H81-DC10:O2	2.161	C9-DC10:C5	2.885	
$[Ru(bpy)_2PIP\text{-}Cl]$	H77-DA9:OP1	1.857	C49-DG12:N7	2.722	22.458
	H76-DA9:OP2	2.0854	C49-DG12:C8	2.456	
	H76-DA9:OP5	2.645	H72-DT8:H71	1.645	
			H71-DT8:H2	1.810	
$[Ru(dmb)_2PIP\text{-}Cl]$	H76-AD15:N3	2.741	C14-DC10:OP1	2.530	18.422
	H77-C10:O2	1.983	C53-DT4:O4	2.702	
	H77-DG13:N3	2.410	H77-DG13:H21	1.497	
	O50-G13:H22	2.048	O50-DG13:O2	1.759	

Table 5 Antibacterial activity of Ru(II) complexes at 20 μg/mL

Complex	Bacterial species	
	E. coli	S. aureus
DMSO	Nil	Nil
$[Ru(phen)_2PIP\text{-}Cl]^{2+}$ (**1**)	15	13
$[Ru(bpy)_2PIP\text{-}Cl]^{2+}$ (**2**)	24	21
$[Ru(dmb)_2PIP\text{-}Cl]^{2+}$ (**3**)	11	10
Septomycine	22	14
Gentamycine	18	18

Zone of inhibition of diameter in (mm)

Staphylococcus aureus (MTCC 96). The experimental results of the compounds were compared against DMSO as the control and are expressed as inhibition zone diameter (in mm) versus control. The standard drugs such as septomycine 5 μg were also tested for their antibacterial activity at the same concentration under the conditions to that of the test compounds. The complex-**2** inhibited the growth of E. coli (24 mm) and S. aureus (21 mm). From the results, it was clear that the inhibition zone of $[Ru(bpy)_2PIP\text{-}Cl]^{2+}$ was higher than the $[Ru(phen)_2PIP\text{-}Cl]^{2+}$ and $[Ru(dmb)_2\ PIP\text{-}Cl]^{2+}$ showed less activity against these bacteria than the standard drug. The activity of the complexes can be explained on the basis of chelation theory. On chelation, the polarity of the metal ion may be reduced to a greater extent due to the overlap of the ligand orbital and partial sharing of the positive charge of the metal ion with donor groups. Further, it increases the delocalization of electrons over the whole chelate ring and enhances the penetration of the complexes into lipid membranes blocking the metal binding sites in the enzymes of microorganisms. These complexes may also disturb the respiration process of the cell and thus block the synthesis of proteins which restricts further growth of the organism [33]. Hence, it may be concluded that Ru(II) complexes will show antimicrobial activity depending on the nature of the ligand.

Conclusions

Three complexes $[Ru(phen)_2PIP\text{-}Cl]^{2+}$, $[Ru(bpy)_2PIP\text{-}Cl]^{2+}$ and $[Ru(dmb)_2PIP\text{-}Cl]^{2+}$ are synthesized and characterized. Spectroscopic studies together with salt-dependent studies and viscosity experiments support that both of the complexes bind to CT-DNA by intercalation via PIP-Cl into the base pairs of DNA. The intrinsic binding constants indicate that $[Ru(phen)_2PIP\text{-}Cl]^{2+}$ binds more avidly to CT-DNA than **2** and **3**. Noticeably, Ru(II) complexes have been found to promote cleavage of plasmid pBR 322 DNA from the supercoiled Form I to the open circular Form II upon irradiation, which may be taken as the potential DNA cleavage reagent.

Acknowledgments We are grateful to the Indian Council for Cultural Relations (ICCR), Hyderabad, for financial support.

References

Arounaguiri S, Maiya BG (1996) Dipyridophenazine complexes of cobalt(III) and nickel(II): DNA-binding and photocleavage studies. Inorg Chem 35:4267–4270

Ashwini Kumar K, Kotha Laxma Reddy, Satyanarayana S (2010) Synthesis, DNA interaction and photocleavage studies of ruthenium(II) complexes with 2-(pyrrole) imidazo[4, 5-f]-1, 10-phenanthroline as an intercalative ligand. J Transition Met Chem 35:713–720

Barton JK, Raphael AL (1984) Photoactivated stereospecific cleavage of double-helical DNA by cobalt(III) complexes. J Am Chem Soc 106:2466–2468

Choi SD, Kim MS, Kim SK, Lincoln P, Tuite E, Norde′n B (1997) Binding Mode of [Ruthenium(II) (1, 10-Phenanthroline)2L]$^{2+}$ with Poly(dT*dA-dT) Triplex. Ligand Size Effect on Third-Strand Stabilization. Biochemistry 36:214–223

Deng H, Cai JW, Xu H, Zhang H, Ji LN (2003) Ruthenium(II) complexes containing asymmetric ligands: synthesis, characterization, crystal structure and DNA-binding. J Chem Soc Dalton Trans 325-330

Devi CS, Nagababu P, Shilpa M, Yata PK, Reddy MR, Gabra NazarMd, Satyanarayana S (2012) Synthesis, characterization and DNA-binding characteristics of Ru(II) molecular light switch complexes. J Iran Chem Soc 9:671–680

Dupureur CM, Barton JK (1997) Structural studies of Λ- and Δ [$Ru(phen)_2dppz]^{2+}$ bound to d(GTCGAC)2: characterization of enantioselective intercalation. Inorg Chem 36:33–43

Graham DR, Marshall LE, Reich KA, Sigman DS (1980) Cleavage of DNA by coordination complexes. Superoxide formation in the oxidation of 1, 10-phenanthroline-cuprous complexes by oxygen - relevance to DNA-cleavage reaction. J Am Chem Soc 102: 5419–5421

Haq I, Lincoln P, Suh D, Norden B, Chowdhry BZ, Chaires JB (1995) Interaction of.DELTA.- and LAMBDA.-[Ru(phen)2DPPZ]$^{2+}$ with DNA: a calorimetric and equilibrium binding study. J Am Chem Soc 117:4788–4796

He X-F, Wang L, Chen H, Lin X, Ji L-N (1998) Synthesis, characterization and dna binding study of Co(III) polypyridyl mixed-ligand complexes. J Polyhdron 18:3161–3166

Hiort C, Lincoln P, Norde′n (1993) B DNA binding of DELTA and LAMBDA -[Ru(phen)2DPPZ]$^{2+}$. J Am Chem Soc 115:3448–3454

Jenkins Y, Friedman AE, Turro NJ, Barton JK (1992) Characterization of dipyridophenazine complexes of ruthenium(II): the light switch effect as a function of nucleic acid sequence and conformation. Biochemistry 13:10809–10816

Jiang CW (2004) Homoleptic ruthenium (II) complexes containing asymmetric tridentate 2-(benzimidazole-2-yl)-1, 10-phenanthroline likes ligands: syntheses, characterization and DNA binding. J Inorg Biochem 98:1399–1404

Jiang CW, Chao H, Lang XL, Li H, Mei WJ, Ji LN (2003) Enantiopreferential DNA-binding of a novel dinuclear complex [$(bpy)_2Ru(bdptb)Ru(bpy)_2]^{4+}$. Inorg Chem Commun 6:773–775

Kratochwil NA, Parkinson JA, Bednarski PJ, Salder PJ (1999) Nucleotide platination induced by visible light. Angew Chem Int Ed Engl 30:1460–1463

Lakowicz JR, Webber G (1973) Quenching of fluorescence by oxygen probe for structural fluctuations in macromolecules. Biochemistry 12:4161–4170

Lecomte JP, Kirsch-De Mesmaeker A, Kelly JM, Tosssi AB, Gorner H (1992) Photo induced electron transfer from mononucleotides to Ruthenium-tris-1,4,5,8-tetraazaphenanthrene: model for photosensitized DNA oxidation. Photochem Photobiol 55(5):681–689

Lincoln P, Norde′n B (1998) DNA binding geometries of ruthenium(II) complexes with 1, 10-phenanthroline and 2, 2′-bipyridyl ligands studied with linear dichroism spectra: borderline cases of intercalation. J Phys Chem B 102:9583

Lincoln P, Broo A, Norde′n B (1996) Diastereomeric DNA-binding geometries of intercalated ruthenium(II) trischelates probed by linear dichroism: $[Ru(phen)_2DPPZ]^{2+}$ and $[Ru(phen)_2BDPPZ]^{2+}$. J Am Chem Soc 118:2644–2653

Liu F, Wang K, Bai G, Zhang Y, Gao L (2004) The pH-induced emission switching and interesting DNA-binding properties of a novel dinuclear ruthenium(II) complex. Inorg Chem 43:1799–1806

Liu Y, Chouai A, Degtyareva NN, Lutterman DA, Dunbar KR, Turro C (2005) Chemical control of the DNA light switch: cycling the switch ON and OFF. J Am Chem Soc 127:10796

Marmur JA (1961) Procedure for the isolation of DNA from microorganisms. J Mol Biol 3:208–218

Morgan RJ, Chatterjee S, Baker AB, Strekas TC (1991) Effects of ligand planarity and peripheral charge on intercalative binding of Ru(2, 2′-bipyridine)$2L^{2+}$ to calf thymus DNA. Inorg Chem 30:2687–2691

Moucheron C, Mesmaeker AKD, Choua C (1997) Photophysics of $Ru(phen)_2(PHEHAT)^{2+}$: a novel "Light Switch" for DNA and photo-oxidant for mononucleotides. Inorg Chem 36:584–592

Mudasir, Wijaya K, Wahyuni ET, Yoshioka N, Inoue H (2006) Salt-dependent binding of iron(II) mixed-ligand complexes containing 1, 10-phenanthroline and dipyrido[3, 2-a:2′, 3′-c]phenazine to calf thymus DNA. Biophys Chem 121:44–50

Nagababu P, Shilpa M, Latha JNL, Bhatnagar I, Srinivas PNBS, Yata PK, Reddy KL, Satyanarayana S (2011) Synthesis, characterization, DNA binding properties, fluorescence studies and toxic activity of cobalt(III) and ruthenium(II) polypyridyl complexes. J Fluores 21:563–572

Perrin D, Annarego WLF, Perrin DR (1980) Purification of laboratory chemicals, 2nd edn. Pergamon, New York

Pyle, A.M, Barton JK, Lippard S.J (1990) Progress in inorganic chemistry bio inorganic chemistry. (ed), John Wiley & Sons, New York. 38: 413-475

Pyle AM, Rehmann JP, Meshoyrer R, Kumar CV, Turro NJ, Barton JK (1989) Mixed-ligand complexes of ruthenium(ii): factors governing binding to DNA. J Am Chem Soc 111:3053

Record MT Jr, Anderson CF, Lohman TM (1978) Thermodynamic analysis of ion effects on the binding and conformational equilibria of proteins and nucleic acids: the roles of ion association or release, screening, and ion effects on water activity. Q Rev Biophys 11:103–178

Rreichmann ME, Rice SA, Thomas CA, Doty P (1954) A further examination of the molecular weight and size of desoxypentose nucleic acid. J Am Chem Soc 76:3047–3053

Satyanarayana S, Dabrowiak JC, Chaires JB (1992) Neither Δ- nor Λ tris(phenanthroline(ruthenium)(II) binds to DNA by classical intercalation. Biochemistry 31:9319–9324

Satyanarayana S, Dabrowiak JC, Chaires JB (1993) Tris (phenanthroline) ruthenium(II) enantiomer interactions with DNA: mode and specificity of binding. Biochemistry 32:2573–2584

Shilpa M, Latha JNL, Gayatri Devi A, Nagarjuna A, Kumar YP, Nagababu P, Satyanarayana S (2011) DNA–interactions of ruthenium(II) & cobalt(III) phenanthroline and bipyridine complexes with a planar aromatic ligand 2-(2-fluronyl)1H-imidazo[4,5-f][1,10-Phenanthroline]. J Incl Phenom Macrocycl Chem 70:187–195

Tan LF, Chao H, Li H, Liu YJ, Sun B, Wei W, LN Ji (2005) Synthesis, characterization, DNA-binding and photocleavage studies of $[Ru(bpy)_2(PPIP)]^{2+}$ and $[Ru(phen)_2(PPIP)]^{2+}$. J inorg Biochem 99:513–520

Wolfe A, Shimer GH, Meehan T Jr (1987) Polycyclic aromatic hydrocarbons physically intercalate into duplex regions of denatured DNA. Biochemistry 26:6392–6396

Xiong Y, Ji LN (1999) Synthesis, DNA-binding and DNA-mediated luminescence quenching of Ru(II) polypyridine complexes. Coord Chem 185:711–733

Xiong Y, He XF, Zou XH, Wu JZ, Chen XM, Ji RH, Li JY, Zhou KB, (1999) Interaction of polypyridyl ruthenium(II) complexes containing non-planar ligands with DNA. J Chem SOC Dalton Trans 1:19-24

Yata PK, Shilpa M, Nagababu P, Reddy MR, Reddy KL, Gabra NazarMd, Satyanarayana S (2012) Study of DNA light switch Ru(II) complexes : synthesis, characterization, photocleavage and antimicrobial activity. J Fluoresc 22:835–847

Zhen QX, Ye BH, Zang QL, Liu JG, Li H, Ji LN, Wang L (1999) Synthesis, characterization and the effect of ligand planarity of $[Ru(bpy)_2L]^{2+}$ on DNA binding affinity. J Inorg Biochem 76:47–53

Zou XH, Ye BH, Li HJ, Liu G, Xiong Y, Ji LN (1999) Mono- and binuclear ruthenium(II) complexes containing a new asymmetric ligand 3-(pyrazin-2-yl)-as-triazino[5,6-f]1,10-phenanthroline: synthesis, characterization and DNA-binding properties. J Chem Soc Dalton Trans 1423–1428